Nanoindentation System for Material Properties Identification

Adrian Wei Hong, Teo, Gik Hong, Yeap, and Wei Jie, Loo

***Abstract*—This paper proposed to design a nanoindentation system with the intention to identify material properties without spalling. The system is designed to perform simulation based on the load-depth curve data collected from NanoTest™. The hardness results are compared with Brinell hardness test and NanoTest™ for the same materials; i.e. brass, mild steel, aluminium and copper. Oliver-Pharr and Joslin-Oliver methods are selected to measure the material properties. Both selected methods require indentation load, impression area and depth to fulfil the material properties calculation while these signals are collected through a displacement sensor and an actuator. The results collected indicate that the spall of material rate, which can be reduced by decreasing the indentation load while maintaining the indentation depth at a longer dwell time. The theoretical simulation result of Joslin-Oliver method which neglects substrate effect acquired an average error rate of 7.823% whereas Oliver-Pharr method acquired an average error rate of 6.355%, both with comparison against NanoTest™ machine. The experiments have been performed using same materials; i.e. brass, aluminium, copper and mild steel.**

***Index Terms*— Nanoindentation, Oliver-Pharr, Joslin-Oliver, Load-depth curve.**

I. Introduction

Hardness indentation test is an essential need towards industry and also to identify the characteristic of the material. Hardness is a material property that defines the resistance between plastic penetration, indentation and deformation. A problem indentation process usually faced is its size scale limitation whereby the size of the indenter exceeds the test material size. Hence, indentation test is designed in different scales from micro to nano with the application of different diamond tip geometry such as Brinell, Vickers and Berkovich. This reduces the risk of material spalling whereby the indentation is performed at small depth and small load. The project is designed with a Nano Indenter II head assembly which includes a displacement sensor, voice coil actuator and diamond Berkovich indenter tip. The designed software implements the preferred Oliver-Pharr method while assuming the material surface is smooth together with Joslin-Oliver method which is able to eliminate substrate effect during indentation test.

Oliver-Pharr method identifies the hardness properties based on area and depth impression acquired during indentation process. This is a popular method as smart vision is not required during the acquisition of the area of indent. However the estimation of contact area based on load-displacement curve can be inaccurate and subsequently affect the calculation of hardness and modulus. Hence, according to Seung et al. [1], indenting the tip within a depth of ~10% of the thin film can resolve this issue which leads to another problem that is the ~10% depth may not be as accurate caused by the specimen surface roughness. The solution to this problem is then referred to Han-Saha hardness which is based on the reduced modulus model by Saha and Nix, E_r(Saha) [2], and used by Han et al. [3] with both based on the assumption of King's flat punch model that is applied on the indenter tip that allows penetration through the film. Joslin-Oliver method in another case, applies to elastically mismatched film whereby it identifies how contact stiffness or modulus is being affected by the increased of indentation depth. The model is as followed:

$$H_{JO} = \frac{P}{A_C} = \beta_i^{\,2} \frac{4}{\pi} \frac{P}{S^2} E_r^{\,2} \tag{1}$$

Where P is load, Ac represents contact area, β_i carries the Berkovich constant value of 1.034, S is stiffness and Er is the reduced modulus.

II. Methodology

A. Oliver-Pharr Method

The designed nanoindentation system is required to measure the hardness and elastic modulus without the need of image capturing, hence the analytical method introduced by Oliver and Pharr is being reviewed due to its adoptability in characterizing small-scale mechanical behaviour [4]. The mechanical properties can be identified based on the load-displacement data acquired at single loading and unloading cycle. However, usual elasticity-based analytic measurement

Manuscript received Nov. 2015, Accepted 2nd December 2015.

"This work was supported in part by the KDU College (PG) Sdn Bhd Internal R&D Fund".

Adrian Wei Hong, Teo was with Department of Engineering, KDU College (PG) Sdn Bhd, 32, Jalan Anson, 10400 Penang, Malaysia. He is now with the National Instruments Southeast Asia Sdn Bhd, No. 8, Lebuh Batu Maung 1, 11900 Bayan Lepas, Penang, Malaysia. (e-mail: adrian.teo@ni.com).

Gik Hong, Yeap, was with Department of Engineering, KDU College (PG) Sdn Bhd, 32, Jalan Anson, 10400 Penang, Malaysia. He is now with the Department of Engineering, KDU University College (PG) Sdn Bhd, 32, Jalan Anson, 10400 Penang, Malaysia. (e-mail: gikhong.yeap@kdupg.edu.my).

Wei Jie, Loo is with the National Instruments Southeast Asia Sdn Bhd, No. 8, Lebuh Batu Maung 1, 11900 Bayan Lepas, Penang, Malaysia. (e-mail: weijie.loo@ni.com).

occurred at the unloading curve which represents the material elastic recovery. The relationship between the depth, h and load, P at the unloading curve is represented as shown [5]:

$$P = \alpha\left(h - h_f\right)^m \tag{2}$$

Where ∝ represents the geometric constants and m represents the theoretical constant value of contact geometry [5]. Parameter maximum displacement, h and final displacement, h_f can be identified through the P-h curve. Elastic deformation between the indenter and test piece is evaluated as the reduced modulus,

$$E_r = \frac{\sqrt{\pi}}{2\beta}\frac{S}{\sqrt{A}} \tag{3}$$

S is obtainable through the unloading of P-h curve whereas contact area, A is calculated through the area function which depends on the indenter scale and geometry [6]. In order to fulfil contact area calculation, the actual indented depth is identified through,

$$h_c = h_t - h_s \tag{4}$$

where h_s is the elastic displacement and can be determined by using Eq (5):

$$h_S = \frac{\varepsilon}{S}P_{\max} \tag{5}$$

h_s can be defined as sink-in of material surface at contact perimeter [5]. The behaviour of the contact depth during unloading and its parameters characterization of contact geometry is as illustrated in Fig. **1**. Furthermore, ε is given as a theoretical value of 0.75 for Berkovich indenter that corresponds to m that varies according to the geometry tip. Lastly, the hardness of the material can be acquired using the equation given by:

$$H = \frac{P_{\max}}{A} \tag{6}$$

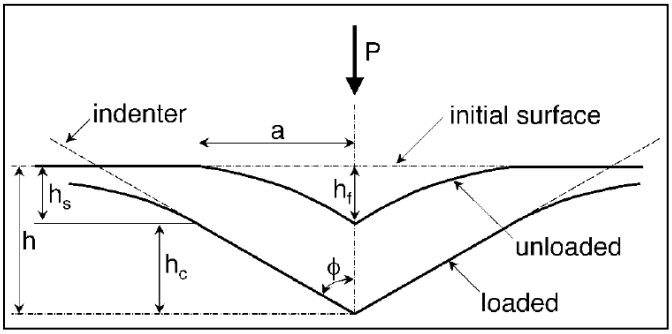

Fig. 1. Unloading parameters of contact geometry.

B. Oliver-Pharr Algorithm Program Flow

During indentation process, it is required to identify the specimen hardness and reduced modulus without the need of visual instruments such as scanning electron microscope (SEM) and atomic force microscopy (AFM), the task needs to be done purely based on the displacement data collected during indentation process. Hence the software of the system is designed to identify each variable required to perform the calculation for hardness by using Eqn (6) and reduced modulus by using Eqn (3).

The program is able to extract specific values from the load-depth curve to identify the indent area with the application of the following formula:

$$A = f\left(h_c\right) = 24.56h_c^{\,2} + 0.562h_c + 0.003216 \tag{7}$$

In this case, C is assumed to be zero, hence acquiring h_c contact depth needs to be estimated based on:

$$h_c = h_t - \frac{\varepsilon}{S}P_{\max} \tag{8}$$

with $\varepsilon = 0.75$ for a paraboloid tip due to the tip selection is diamond Berkovich. Though the contact depth is needed for the area measurement, stiffness, S is also required to fulfil the calculation as well. Therefore the formula as shown below is prioritized before proceeding to hardness and reduced modulus measurement.

$$S = \frac{dP}{dh} = \frac{P_{\max}}{h_t - h_f} \tag{9}$$

The following stiffness calculation is based on the upper 30% - 40% of unloading curve which stated by Qianhua Kan et al that this allows a more effective reduced modulus calculation as compared to 25% - 50% suggested by Hay and Pharr [4, 7].

C. DAQ Hardware and Software

National Instruments myRIO-1900 is chosen as the data acquisition hardware and controlling system for the project due to its suitable output voltage required for supplying the actuator and controlling the load. In addition, it also consists of analogue input pin that allows displacement signal acquisition. Moreover, the device is small in dimension which meets the portability requirement and it is programmed by using NI LabVIEW DAQ software [8].

National Instruments LabVIEW is an analytical design and measurement software which consist of controlling capabilities and also runs in graphical programming interface that allows ease of signal monitoring and processing. Furthermore, the software platform is designed to control as a stand-alone instrument which is capable at running in

automated real-time system [9].

D. Voice Coil Actuator

The Voice coil actuator is designed with a permanent magnet and coil winding as a conductor which allows limited motion according to the current applied to the conductive coil which is proportional to the output force produced. Voice coil actuator can be designed in linear motion and the force can be varied according to input current as well. The selected voice coil actuator is integrated in the head assembly together with a build in capacitive displacement sensor.

Voice coil actuator holds a simple construction with no gears included as compared to motor actuator. The force produced by the actuator varies directly from the current supplied due to the constant electrical resistance of the coil. However, during indentation process, higher force is required to act against the specimen hence the actuator itself draws larger current to oppose the indentation force [10].

III. Experiment and Results

The nanoindentation system designed in this project consists of a main controller, indenter head assembly, aluminium frame and stainless steel adjustable stage. Fig. **2** illustrates the hardware of the nanoindentation system.

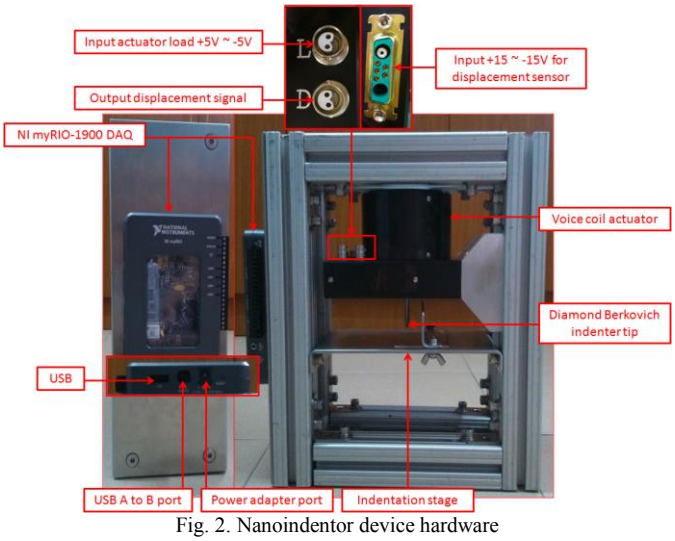

Fig. 2. Nanoindentor device hardware

The main controller of the system used is National Instruments myRIO-1900 data acquisition hardware which allows communication between LabVIEW that performs the I/O data acquisition from the indenter head assembly. On the other hand, the head assembly contains a voice coiled actuator which produces current in the coil assembly when load coaxial port is connected and controlled within +5 to -5 V. This causes the coil to be either pull towards the internal permanent magnet or push away, depending on the load voltage.

Furthermore, the head assembly also consists of a displacement sensor which reads the movement of the actuator tip by a 3 plate capacitive gauge. The measurement of the sensor requires a positive and negative voltage of 15 V which is connected to the female D-sub connector. Another important feature of the system is the indentation stage where its height is adjustable according to the size of the specimen.

A. Brinell Hardness Test

The material properties recorded from the following Brinell experiment has been divided into two different loading for comparison purpose as shown in TABLE 1 and TABLE 2.

TABLE 1
BRINELL HARDNESS MEASUREMENT WITH 30kN LOAD

Force (N)	Test Piece	Copper			Aluminum			Brass			Mild Steel		
	Trials	1	2	3	1	2	3	1	2	3	1	2	3
30000	Diameter of indentation (mm)	6.5	6.7	6.4	6.4	6.3	6.7	6.3	6.3	6.0	5.5	5.6	5.6
	Average diameter (mm)	6.533			6.467			6.200			5.567		
	Brinell Hardness (BHN)	80.167			82.094			90.413			115.056		

TABLE 2
BRINELL HARDNESS MEASUREMENT WITH 20kN LOAD

Force (N)	Test Piece	Copper			Aluminum			Brass			Mild Steel		
	Trials	1	2	3	1	2	3	1	2	3	1	2	3
20000	Diameter of indentation (mm)	5.2	5.4	5.2	5.6	5.6	5.7	4.9	5.0	5.0	4.0	4.1	3.8
	Average diameter (mm)	5.267			5.633			4.967			3.967		
	Brinell Hardness (BHN)	86.596			74.715			98.314			158.260		

30 kN loading force shows a promising result whereby the BHN acquired are within the range of typical soft brass and mild steel material hardness. Mild steel holds the highest BHN while copper holds the least, due to brass is a composite comprised with copper and zinc which makes it harder compared to copper. As for the 20 kN loading experiment, the results are slightly off and this may be caused by several predicted factors:

1. Surface roughness affects the Brinell hardness test.
2. Indentation taken too close to the edge causes side bulging that affects the results.
3. The indentation does not meet the required depth of impression.

From the 3 factors listed above, it is more likely that the inaccurate results is due to the depth of impression during indentation. Hence, the indentation depth needed is estimated by using the following formula:

$$t = \frac{1}{2}\left[D - \sqrt{D^2 - d^2}\right] \tag{10}$$

$$t = \frac{P}{BHN \times \pi \times D} \tag{11}$$

Equation (10) is used to calculate the depth by using existing diameter of indentation whereas (11) is used to calculate based on the 30kN hardness results under 20kN calculation to predict the required indentation depth to achieve approximate similar hardness. The error rate between the achieved depth of impression and estimated depth of impression under 20kN has been estimated as shown in TABLE 3

TABLE 3
DEPTH OF IMPRESSION MEASUREMENT

Force (N)	Test Piece	Copper	Aluminum	Brass	Mild Steel
30000	Depth of impression (mm)	1.215	1.186	1.077	0.846
20000	Depth of impression (mm)	0.750	0.869	0.660	0.410
	Expected depth from 20kN load	0.810	0.791	0.718	0.564
	Error rate (%)	7.425	9.876	8.036	27.299

The results acquired in Table show that mild steel carries the highest error rate of 27.299%. Two hypotheses have been made from this occurrence: 1. The high elasticity of mild steel causing the dwell time of 15 seconds is too short to build the expected impression depth/plastic depth (h_f), causing a high contact depth (h_c) to occur during the unloading of the tip. 2. The supplied load of 20 kN is not enough to penetrate the material to its desired impression depth. In order to acquire more accurate results when using 30 kN load, the dwell time needs to be taken into consideration where the depth of impression varies whenever the dwell time extends.

This experiment is able to conclude that loading timing profile holds an important role during a hardness indentation process and this may affect the accuracy of the final hardness results. Therefore, by designing a user friendly loading timing profile, it increases the flexibility to vary the impression depth during indentation process.

B. Simulation – Oliver-Pharr

The simulation conducted utilizes data extracted from NanoTest™ results acquired from similar materials. During NanoTest™ nanoindentation test, a load-displacement signal is acquired and the values obtained for the simulation are as shown in Fig. **3**. The circled points in the graph representing the maximum load, maximum depth and plastic depth.

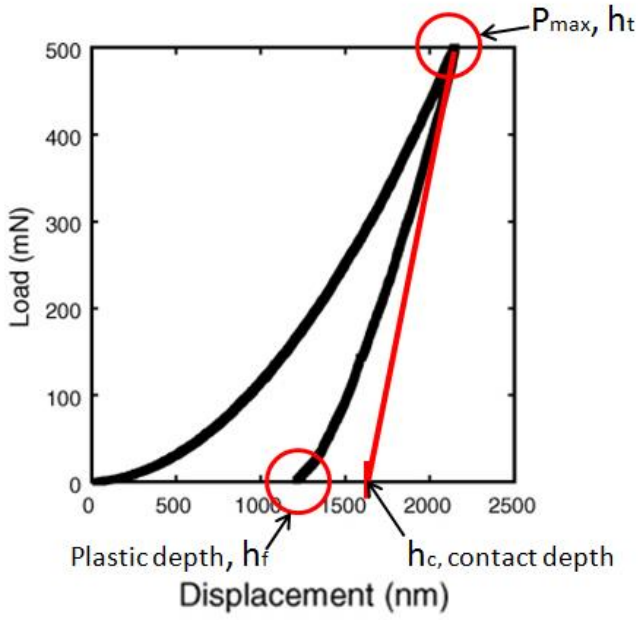

Fig. 3. Load-displacement curve - data extraction

The Oliver-Pharr hardness derivation is performed as shown:

$$H_{OP} = \frac{P_{max}}{24.56\left[h_t - \frac{\varepsilon}{\left(\frac{P_{max}}{h_t - h_f}\right)} \times P_{max}\right]^2 + 0.562\left[h_t - \frac{\varepsilon}{\left(\frac{P_{max}}{h_t - h_f}\right)} \times P_{max}\right] + 0.003216}$$

$$= \frac{P_{max}}{24.56\left[h_t - \frac{\varepsilon(h_t - h_f)}{P_{max}} \times P_{max}\right]^2 + 0.562\left[h_t - \frac{\varepsilon(h_t - h_f)}{P_{max}} \times P_{max}\right] + 0.003216}$$

$$= \frac{\boldsymbol{P_{max}}}{24.56[\boldsymbol{h_t}(1-\varepsilon) + \varepsilon \boldsymbol{h_f}]^2 + 0.562[\boldsymbol{h_t}(1-\varepsilon) + \varepsilon \boldsymbol{h_f}] + 0.003216} \quad (12)$$

Where Hop represents Oliver-Pharr hardness, h_f is the plastic depth, ht is the maximum depth and Pmax is the maximum load. During Oliver-Pharr measurement, the material surface is assumed to be smooth and does not pile-up or sink-in during indentation. The variables for hardness calculation are as illustrated in Fig. **4**.

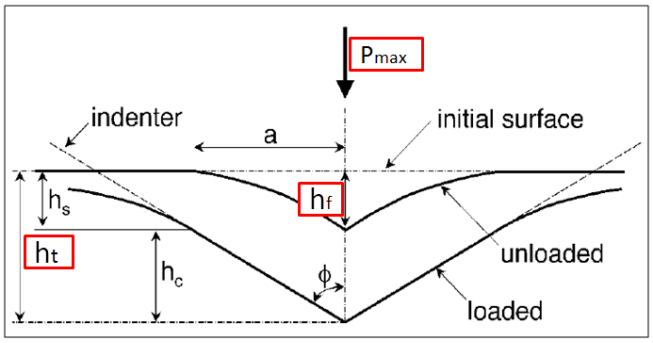

Fig. 4. Highlighted variable needed for hardness calculation

C. Simulation – Joslin-Oliver

The Joslin-Oliver method holds an advantage to nanoindentation where it eliminate substrate effect while assuming the indentation depth does not affecting the reduced modulus, E_r, whereby it is at fix state. The hardness can be calculated based on the formula as shown:

$$H_{JO} = \frac{4\beta^2}{\pi} \times \frac{P_{max}}{S^2} \times E_r^{\,2} \quad (13)$$

Where S, stiffness can be acquired based on Eqn (9), reduced modulus, E_r from Eqn (3) and β = 1.034 constant value for Berkovich indenter tip.

TABLE 4 shows the recorded hardness results for the four materials where copper with 1.508 GPa, aluminium with the lowest GPa of 1.323, brass with the second highest GPa of 2.879 and lastly, mild steel with the highest hardness GPa average value of 3.105. In summary, the hardness sequence for the material in this experiment is proven correct, but slightly higher as compared to Oliver-Pharr method due to the assumption of reduced modulus being constant.

TABLE 4
JOSLIN-OLIVER METHOD 4 MATERIALS SIMULATION RESULTS

Copper	**Reduced Modulus**	9.250	8.892	9.115	9.533	9.344
	Hardness (GPa)	1.595	1.409	1.466	1.564	1.505
	Hardness (HV)	162.620	143.636	149.464	159.496	153.436
	Average Hardness (GPa)	**1.508**				
	Average Hardness (HV)	**153.730**				
Aluminum	**Reduced Modulus**	4.811	4.687	4.763	4.878	4.791
	Hardness (GPa)	1.358	1.294	1.267	1.307	1.390
	Hardness (HV)	138.465	131.928	129.210	133.232	141.775
	Average Hardness (GPa)	**1.323**				
	Average Hardness (HV)	**134.922**				
Brass	**Reduced Modulus**	6.962	6.503	6.779	6.779	-
	Hardness (GPa)	2.721	2.776	2.785	3.234	-
	Hardness (HV)	277.449	283.042	283.992	329.787	-
	Average Hardness (GPa)	**2.879**				-
	Average Hardness (HV)	**293.567**				-
Mild steel	**Reduced Modulus**	14.293	12.633	15.240	5.632	14.718
	Hardness (GPa)	3.133	3.435	3.107	2.952	2.900
	Hardness (HV)	319.515	350.243	316.865	300.990	295.675
	Average Hardness (GPa)	**3.105**				
	Average Hardness (HV)	**316.658**				

D. Simulation – LabVIEW Interface

Each experiment is performed using LabVIEW software where the program is able to control the pins of myRIO-1900 DAQ directly while acquiring data for material hardness measurement. Fig. **5** shows the first page of the program where it allows user to control the load timing with the objective to increase depth while reducing its load. It also simultaneously acquire the displacement signals as well.

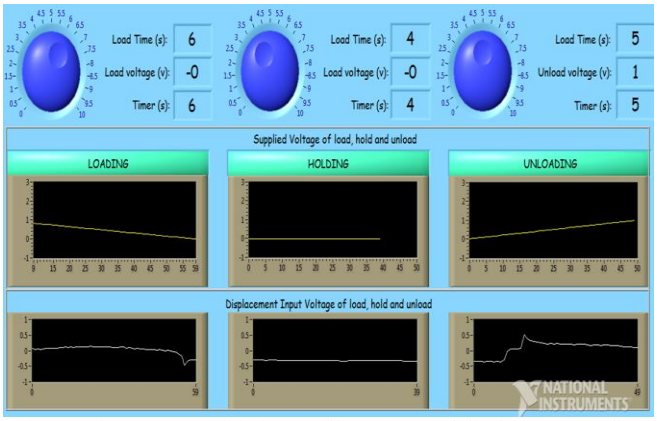

Fig. 5. LabVIEW - Load timing profile settings and displacement reading

Fig. **6** provides another option to the user by inserting total depth, plastic depth and maximum load parameters for hardness calculation through Oliver-Pharr and Joslin-Oliver method. This feature allows flexibility towards comparison between different algorithms throughout the experiment.

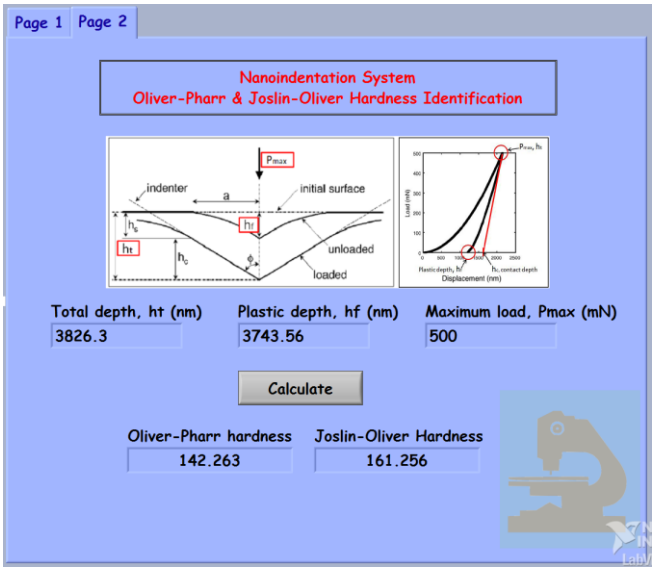

Fig. 6. LabVIEW - Oliver-Pharr & Joslin-Oliver hardness acquisition

IV. Discussions and Comparisons

The aim of the comparison is to acquire minimal error rate nanoindentation technique to be implemented in the nanoindentation system.

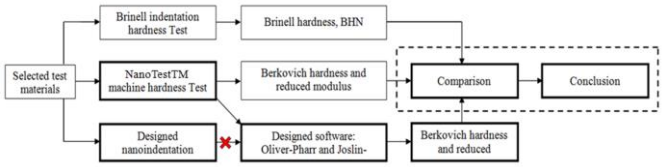

Fig. 7. Experiment block – results comparison

As shown in Fig. **7**, the first comparison includes Brinell test, NanoTest™, simulation test based on Oliver-Pharr method and Joslin-Oliver method. The results is tabulated in TABLE 5. Due to Brinell is not under nanoindentation category, its hardness values are converted to Mohs for comparison purpose. Therefore, copper held a Mohs hardness value at the range of 2 – 2.5 whereas Oliver-Pharr hardness is at the range of 2.7 – 2.8. Joslin-Oliver consists of a larger range compared to Brinell hardness which may be caused by Brinell test inconsistency of reduced modulus value. Furthermore, mild steel for Brinell test holds a Mohs value range of 2.7 – 2.8, which may cause reading error against copper readings from Oliver-Pharr method. Hence, Mohs hardness conversion value is not suitable to perform comparison between indentation and nanoindentation hardness.

TABLE 5
COMPARISON BETWEEN BRINELL, NanoTest™ AND LabVIEW SOFTWARE SIMULATION HARDNESS RESULTS

	Comparison	Hardness			
		Indentation	Nanoindentation		
		Brinell Test	NanoTest TM	Simulation (Oliver-Pharr)	Simulation (Joslin-Oliver)
Materials	Copper	80.167	140.249	134.486	153.730
	Aluminum	82.094	126.567	118.032	134.922
	Brass	90.413	267.685	245.452	293.567
	Mild Steel	115.056	292.864	277.018	316.658

TABLE 6 compared between NanoTest™ machine hardness estimation and the simulation software based Oliver-Pharr method, with an average error rate of 6.355% however the hardness sequence of the material is still correct.

TABLE 6
NanoTest™ VS SIMULATION (OLIVER-PHARR) HARDNESS

	Comparison	Nanoindentation		Error Rate (%)
		NanoTest TM	Simulation (Oliver-Pharr)	
Materials	Copper	140.249	134.222	4.297
	Aluminum	126.567	117.645	7.049
	Brass	267.685	244.494	8.664
	Mild Steel	292.864	277.018	5.411
			Average Error Rate (%)	6.355

As for the comparison between NanoTest™ and Joslin-Oliver method, the machine identifies the hardness by accepting every factor that may affect the results including the substrate effect, while Joslin-Oliver eliminates the substrate effect by assuming the reduced modulus is constant. Therefore the final calculation results in an error rate of 7.823%, which is higher than Oliver-Pharr method as shown in TABLE 7.

TABLE 7
NanoTest™ VS SIMULATION (JOSLIN-OLIVER) HARDNESS

	Comparison	Nanoindentation		Error Rate (%)
		NanoTest TM	Simulation (Joslin-Oliver)	
Materials	Copper	140.249	153.730	8.769
	Aluminum	126.567	134.922	6.193
	Brass	267.685	293.567	8.816
	Mild Steel	292.864	316.658	7.514
			Average Error Rate (%)	7.823

From the Brinell test, it is observable that the time of indentation defines the depth and area of the indent impression which may affect the hardness results. On the other hand, nanoindentation aims to reduce material used and avoid spalling of material. In this case, Brinell test is able to reduce its indentation depth by reducing the load while increasing the dwell time. This is to form a better impression depth in order to achieve a desired area to measure the hardness of the material. This not only reduces the area of indent but also allows Brinell test to be performed on thinner materials. Furthermore, the nanoindentation tests and its comparison are able to conclude that there are still many parameters needs to be considered while measuring the hardness at nano scale. These factors include gravity, material's surface roughness and environment sound frequency which may cause vibrations.

V. CONCLUSION

The project concludes the essentiality of acquiring a smart vision scope which allows the user to identify substrate error or indentation error which might affect the results. It is advisable to construct a nanoindentation system using separated components due to the sensitivity of actuator and displacement sensor. Avoid using glass made capacitive displacement sensor that can be broken easily. Instead, opt for laser sensor which is able to produce the desired output. While constructing the nanoindentation system, precision X-Y axis motorized stage is able to allow the indentation to take place with small range in between that saves space and material which meets the main intension of a nanoindentation system. As to avoid vibration emitted from the ground, magnetic floating table can be implemented to reduce the error rate during nanoindentation process. Last but not least, the project experiment may also concludes that the criticalness of dwell time during indentation will affect the depth of impression and subsequently resulting in false measurement of the hardness of the materials.

ACKNOWLEDGMENT

We would like to thank National Instruments for providing the software license and DAQ hardware to complete the construction of the nanoindentation system. We also would like to thank Ms Lian Li Hung for proof reading this paper.

REFERENCE

[1] S. M. Han, "Extracting thin film hardness of extremely compliant films on stiff substrates," *Thin Solid Films,* vol. 519, no. 10, pp. 3221-3224, 1 March 2011.

[2] R. Saha, "Effects of the substrate on the determination of thin film mechanical properties by nanoindentation," *Acta Materialia,* vol. 50, no. 1, pp. 23-38, January 2002.

[3] S. M. Han, "Determining hardness of thin films in elastically mismatched film-on-substrate systems using nanoindentation," *Acta Materialia,* vol. 54, no. 6, pp. 1571-1581, April 2006.

[4] W.C. Oliver and G. M. Pharr "Measurement of hardness and elastic modulus by instrumented indentation: Advances in understanding and refinements to methodology," *Journal of Materials Research*, vol. 19, no.1, pp. 3-20, January 2004.

[5] M. R. VanLandingham, "Review of Instrumented Indentation," *Journal of Research of the National Institute of Standards and Technology,* vol. 108, no. 4, pp. 249-265, July-August 2003.

[6] J. Hay, "Introduction to Instrumented Indentation Testing," *Experimental Techniques,* vol. 33, no. 6, pp. 66-72, November/December 2009.

[7] Q. Kan, W. Yan, G. Kang and Q. Sun, "Oliver–Pharr indentation method in determining elastic moduli of shape memory alloys - A phase transformable material," Journal of the Mechanics and Physivs of Solids, vol. 61, no. 10, pp. 2015 - 2033, October 2013.

[8] "Ni myRIO-1900 User Guide and Specifications," ed: National Instruments.

[9] *Top 10 Reasons to Use LabVIEW for Acquiring Data and Processing Signals*. Available: http://www.ni.com/white-paper/9080/en/

[10] G. Gogue. *Voice-Coil Actuator*. Available: http://www.consult-g2.com/papers/paper8/paper.html

Adrian Wei Hong, Teo received Bachelor degree in Electrical and Electronic Engineering from Northumbria University, UK in 2015.
Mr Adrian has been awarded 1st Runner up in Schneider Electric Go Green in the City Competition 2015 for South East Asia region, Champion of Malaysia Stage in Schneider Electric Go Green in the City Competition 2015, 2nd Runner up in IHL-MSC Malaysia Startup Challenge, 2nd Runner up in Innovate Malaysia National Instruments track and was a recipient of the International Colloquium on Textile Engineering, Fashion, Apparel and Design Conference.

Gik Hong, Yeap received his Diploma in Mechanical Engineering from Sultan Abdul Halim Mu'adzam Shah Polytechnic (POLIMAS), Jitra, Kedah in 2001. Received his BEng (Hons) Mechanical Engineering and Manufacturing Systems from the University of Lincoln, UK in 2003 with First Class Honours. He later obtained his MSc Advanced Materials and Manufacturing from the University of Hull, UK in 2006 with Distinction. In September 2005, he was awarded the PhD Studentship and obtained his PhD in Electronics Engineering degree from the University of Hull, UK in 2010. He is a Member of the Institute of Engineering and Technology (IET), UK, a Graduate Member of Institute of Engineers Malaysia (IEM) and Graduate Engineers of Board of Engineers Malaysia (BEM). He is also a committee member of Malaysia TRIZ Innovation Association (MyTRIZ). He is a certified MyTRIZ Level 3 Practitioner and MyTRIZ Level 1 Instructor.

He joined KDU College (PG) Sdn Bhd in December 2009 as a lecturer and subsequently being promoted as the Programme Leader in August 2010 before take on the role of Academic Department Head of Engineering Department in the School of Engineering, Science and Technology at KDU College Penang in June 2013.

Besides the administrative and academic responsibilities, Dr Yeap is also active in research. He has published a number of journals and conference papers in the renowned international journals and conferences. His research interests include physics of semiconductor, robotics, renewable energy, industrial automation, etc.

Wei Jie, Loo graduated with Bachelor's Degree in Engineering majoring in Mechatronic Engineering from UCSI University, Malaysia. He joined National Instruments in 2011 as an Applications Engineer where he provides technical support to customers across the ASEAN region, assisting sales in accomplishing complex opportunities using NI platform and conducts training and seminars on a variety of NI software and hardware products.

He was then promoted to Field Application Engineer in 2012 and is currently the Field Sales Engineer serving customers in the Northern Region of Malaysia which includes Perak, Kedah, Perlis, Kelantan and parts of Penang. He also conducts customer education courses in LabVIEW applications and various seminars in ASEAN regularly.